Cancer Cell, Volume *39*

Supplemental information

Single-cell analysis defines a pancreatic fibroblast lineage that supports anti-tumor immunity

Colin Hutton, Felix Heider, Adrian Blanco-Gomez, Antonia Banyard, Alexander Kononov, Xiaohong Zhang, Saadia Karim, Viola Paulus-Hock, Dale Watt, Nina Steele, Samantha Kemp, Elizabeth K.J. Hogg, Joanna Kelly, Rene-Filip Jackstadt, Filipa Lopes, Matteo Menotti, Luke Chisholm, Angela Lamarca, Juan Valle, Owen J. Sansom, Caroline Springer, Angeliki Malliri, Richard Marais, Marina Pasca di Magliano, Santiago Zelenay, Jennifer P. Morton, and Claus Jørgensen

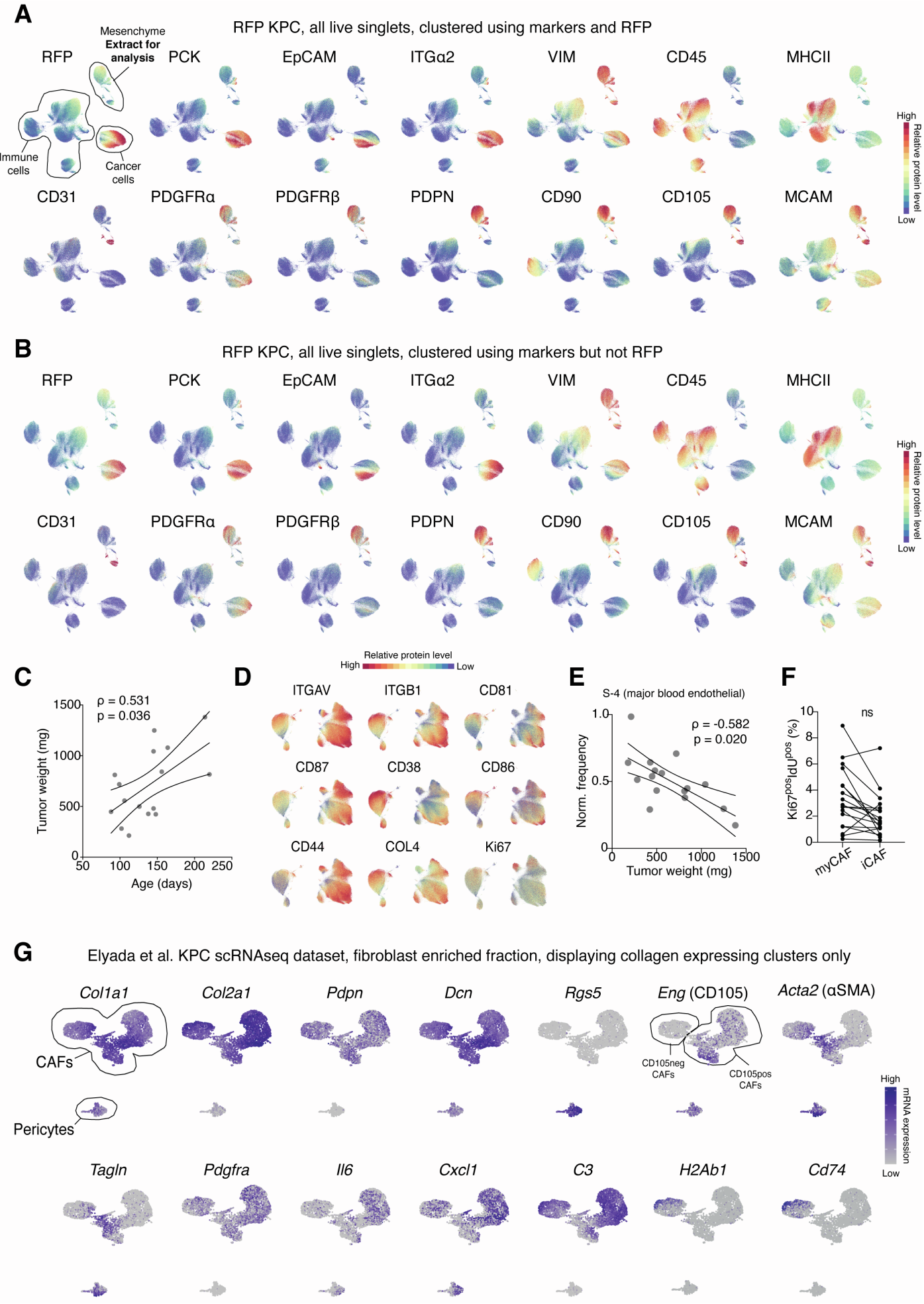
A
RFP KPC, all live singlets, clustered using markers and RFP
Mesenchyme
Extract for analysis
Immune cells
Cancer cells
RFP
PCK
EpCAM
ITGα2
VIM
CD45
MHCII
CD31
PDGFRα
PDGFRβ
PDPN
CD90
CD105
MCAM
High
Relative protein level
Low
B
RFP KPC, all live singlets, clustered using markers but not RFP
RFP
PCK
EpCAM
ITGα2
VIM
CD45
MHCII
CD31
PDGFRα
PDGFRβ
PDPN
CD90
CD105
MCAM
High
Relative protein level
Low
C
ρ = 0.531
p = 0.036
Tumor weight (mg)
Age (days)
D
Relative protein level
High
Low
ITGAV
ITGB1
CD81
CD87
CD38
CD86
CD44
COL4
Ki67
E
S-4 (major blood endothelial)
ρ = -0.582
p = 0.020
Norm. frequency
Tumor weight (mg)
F
ns
Ki67posIdUpos (%)
myCAF
iCAF
G
Elyada et al. KPC scRNAseq dataset, fibroblast enriched fraction, displaying collagen expressing clusters only
Col1a1
Col2a1
Pdpn
Dcn
Rgs5
Eng (CD105)
Acta2 (αSMA)
CAFs
CD105neg CAFs
CD105pos CAFs
Pericytes
High
mRNA expression
Low
Tagln
Pdgfra
Il6
Cxcl1
C3
H2Ab1
Cd74

Supplemental Figure 1, related to Figure 1. Phenotypic and compositional heterogeneity of pancreatic cancer-associated mesenchymal cells

(A) UMAP projection of all live, single cells from an RFP KPC tumor sample using all phenotypic markers to drive clustering. PCK: pan-cytokeratin.

(B) UMAP projection of all live, single cells from an RFP KPC tumor sample, as for (A), but RFP is not used to drive clustering. PCK: pan-cytokeratin.

(C) Correlation between KPC mouse age and weight of tumors collected at humane endpoint. ρ=Spearman correlation coefficient, 90% confidence intervals displayed. Mean age of mice included in study was 142 days.

(D) UMAP projection from Figure 1A, displaying relative signal intensity of additional phenotypic markers not included in Figure 1D.

(E) Spearman correlation analysis between the relative frequency of the endothelial cell subset, S-4 and PDA tumor weight. ρ=Spearman correlation coefficient, 90% confidence intervals displayed.

(F) Frequency of myCAFs (αSMA^{high} PDGFRα^{low}) and iCAFs (αSMA^{low} PDGFRα^{high}) in S-phase (Ki67^{pos} IdU^{pos}).

(G) Reanalysis of single cell transcriptomic data from Elyada et al. The pre-defined fibroblast enriched fraction was used and only collagen expressing cells analyzed. Data is displayed as UMAP projections with overlaid relative expression levels of example genes, including canonical fibroblast genes (*Col1a1/2*, *Pdpn*, *Dcn*), the canonical pericyte gene (*Rgs5*), *Eng* (the gene that encodes CD105) and myCAF-, iCAF- and apCAF-associated genes (*Acta2*, *Tagln* and *Pdgfra*, *Il6*, *Cxcl1*, *C3*, and *H2Ab1*, *Cd74* respectively).

Samples are compared using Spearman correlation adjusted for multiple testing using Benjamini-Hochberg correction (C, E) or paired t-test (F). ns. non-significant

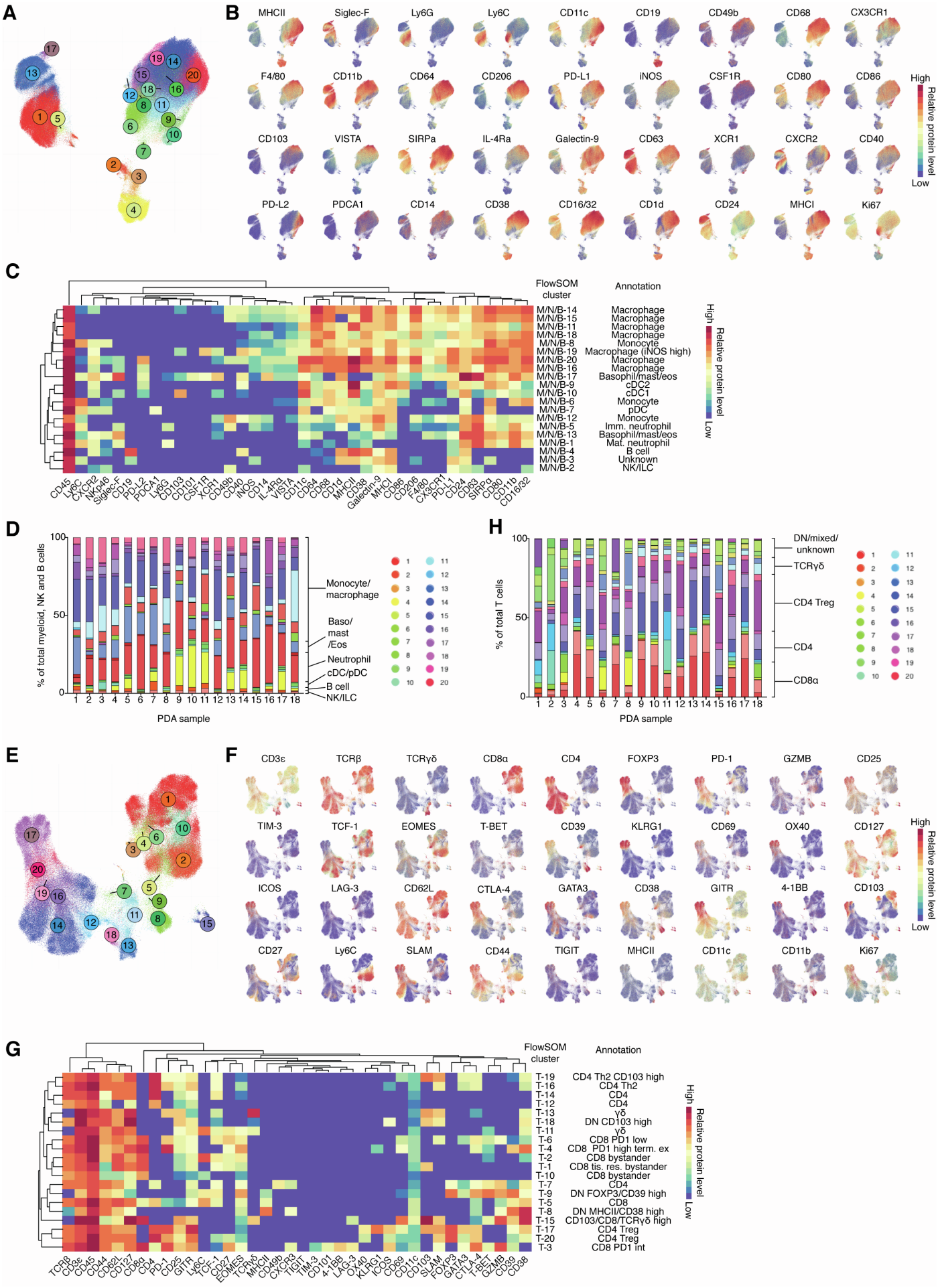
A
B
MHCII
Siglec-F
Ly6G
Ly6C
CD11c
CD19
CD49b
CD68
CX3CR1
F4/80
CD11b
CD64
CD206
PD-L1
iNOS
CSF1R
CD80
CD86
CD103
VISTA
SIRPa
IL-4Ra
Galectin-9
CD63
XCR1
CXCR2
CD40
PD-L2
PDCA1
CD14
CD38
CD16/32
CD1d
CD24
MHCI
Ki67
High
Relative protein level
Low
C
FlowSOM cluster
Annotation
M/N/B-14 Macrophage
M/N/B-15 Macrophage
M/N/B-11 Macrophage
M/N/B-18 Macrophage
M/N/B-8 Monocyte
M/N/B-19 Macrophage (iNOS high)
M/N/B-20 Macrophage
M/N/B-16 Macrophage
M/N/B-17 Basophil/mast/eos
M/N/B-9 cDC2
M/N/B-10 cDC1
M/N/B-6 Monocyte
M/N/B-7 pDC
M/N/B-12 Monocyte
M/N/B-5 Imm. neutrophil
M/N/B-13 Basophil/mast/eos
M/N/B-1 Mat. neutrophil
M/N/B-4 B cell
M/N/B-3 Unknown
M/N/B-2 NK/ILC
CD45 Ly6C CXCR2 NKp46 Siglec-F CD19 PD-L2 PDCA1 Ly6G CD103 CD101 CSF1R XCR1 CD49b CD40 iNOS CD14 IL-4Ra VISTA CD11c CD64 CD68 CD1d MHCII CD38 Galectin-9 MHCI CD86 CD206 F4/80 CX3CR1 PD-L1 CD24 CD63 SIRPa CD80 CD11b CD16/32
D
% of total myeloid, NK and B cells
PDA sample
Monocyte/ macrophage
Baso/ mast /Eos
Neutrophil
cDC/pDC
B cell
NK/ILC
H
% of total T cells
PDA sample
DN/mixed/ unknown
TCRγδ
CD4 Treg
CD4
CD8α
E
F
CD3ε TCRβ TCRγδ CD8α CD4 FOXP3 PD-1 GZMB CD25
TIM-3 TCF-1 EOMES T-BET CD39 KLRG1 CD69 OX40 CD127
ICOS LAG-3 CD62L CTLA-4 GATA3 CD38 GITR 4-1BB CD103
CD27 Ly6C SLAM CD44 TIGIT MHCII CD11c CD11b Ki67
High
Relative protein level
Low
G
FlowSOM cluster
Annotation
T-19 CD4 Th2 CD103 high
T-16 CD4 Th2
T-14 CD4
T-12 CD4
T-13 γδ
T-18 DN CD103 high
T-11 γδ
T-6 CD8 PD1 low
T-4 CD8 PD1 high term. ex
T-2 CD8 bystander
T-1 CD8 tis. res. bystander
T-10 CD8 bystander
T-7 CD4
T-9 DN FOXP3/CD39 high
T-5 CD8
T-8 DN MHCII/CD38 high
T-15 CD103/CD8/TCRγδ high
T-17 CD4 Treg
T-20 CD4 Treg
T-3 CD8 PD1 int
TCRβ CD3ε CD45 CD44 CD62L CD127 CD8α CD4 PD-1 CD25 GITR Ly6C TCF-1 CD27 EOMES TCRγδ MHCII CD49b CXCR3 TIGIT TIM-3 CD101 4-1BB LAG-3 OX40 KLRG1 ICOS CD69 CD11c CD103 SLAM FOXP3 GATA3 CTLA-4 T-BET GZMB CD39 CD38
High
Relative protein level
Low

Supplemental Figure 2, related to Figure 2. Phenotypic and compositional heterogeneity of pancreatic cancer-associated immune subsets

(A) UMAP projection of single $CD45^{pos}$ $CD3^{neg}$ cells (MNB: Myeloid, NK, B cell) from 18 of the 19 tumors analyzed for the mesenchymal stroma with color-coded FlowSOM clusters (1-20). Each sample contributes an equal number of cells to the dataset. Total of $5x10^5$ cells displayed.

(B) UMAP projection (from (A)) displaying overlaid relative signal intensity of example phenotypic markers.

(C) Heatmap of marker median mass intensities (MMIs) displayed as z-scores. Each FlowSOM MNB cluster is grouped by unsupervised hierarchical clustering based on marker MMIs. Cell-type annotations based on canonical phenotypic markers are listed.

(D) Stacked bar graph displaying relative abundance of KPC PDA MNB FlowSOM clusters grouped into major MNB cell sub-types.

(E) UMAP projection of single $CD45^{pos}$ $CD3^{pos}$ cells (T cells) from 18 of the 19 tumors analyzed for the mesenchymal stroma with color-coded FlowSOM clusters (1-20). Each sample contributes an equal number of cells to the dataset. Total of $5x10^5$ cells displayed.

(F) UMAP projection from (E) displaying overlaid relative signal intensity of example phenotypic markers.

(G) Heatmap of marker median mass intensities (MMIs) displayed as z-scores. Each FlowSOM T cell cluster is grouped by unsupervised hierarchical clustering based on marker MMIs. Cell-type annotations based on canonical phenotypic markers are listed.

(H) Stacked bar graph displaying relative abundance of KPC PDA T cell FlowSOM clusters grouped into major T cell sub-types.

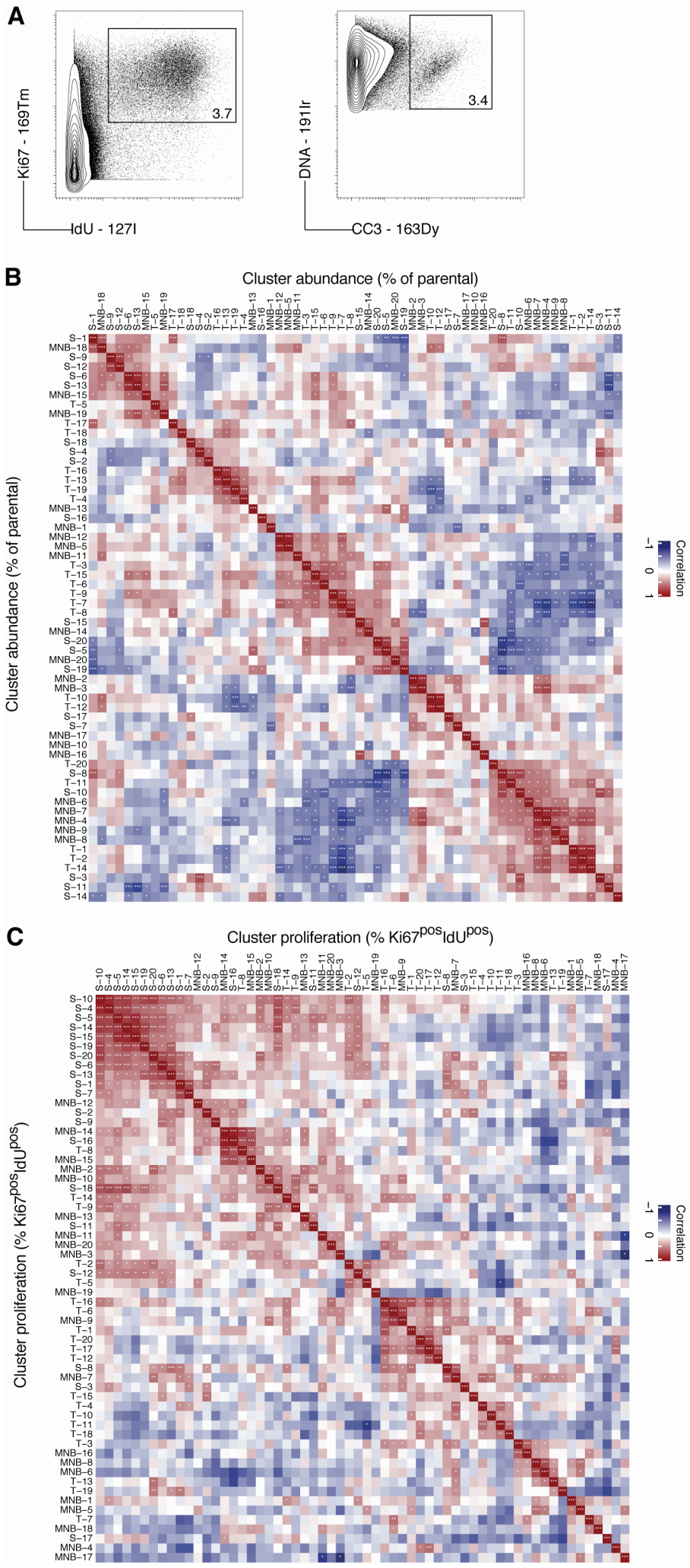
A
Ki67 - 169Tm
IdU - 127I
3.7
DNA - 191Ir
CC3 - 163Dy
3.4
B
Cluster abundance (% of parental)
Cluster abundance (% of parental)
Correlation
C
Cluster proliferation (% Ki67posIdUpos)
Cluster proliferation (% Ki67posIdUpos)
Correlation

Supplemental Figure 3, related to Figure 2. Co-regulated CAF and immune subsets within the PDA tumor microenvironment

(A) Example mass cytometry (MC) data with Ki67 and IdU (left) and DNA and cleaved caspase-3 (CC3) (right). Cells in S-phase, at the time the tumor was collected, can be clearly identified as $Ki67^{pos}$ IdU^{pos} and apoptotic cells as $CC3^{pos}$.

(B-C) Correlation matrix with Spearman correlation coefficients of all pairwise comparisons of mesenchymal stromal and immune cell subset frequencies (B) and proliferation rates (C). All pairwise apoptosis rate correlations are included in Table S2.

Samples were compared using Spearman correlation adjusted for multiple testing using Benjamini-Hochberg correction (J,K). *p<0.05, **p<0.01, ***p<0.001.

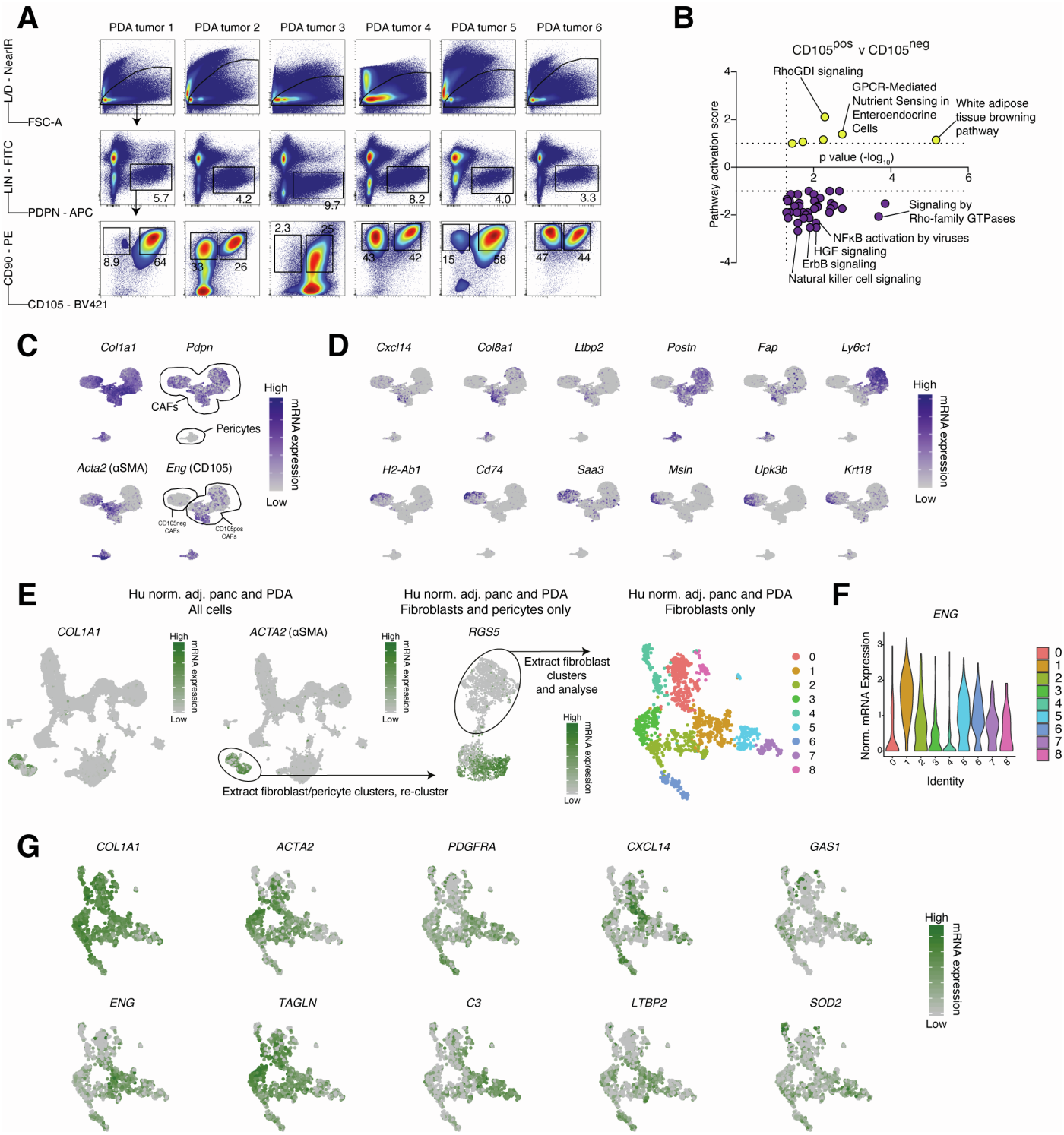
A
PDA tumor 1
PDA tumor 2
PDA tumor 3
PDA tumor 4
PDA tumor 5
PDA tumor 6
L/D - NearIR
FSC-A
LIN - FITC
PDPN - APC
CD90 - PE
CD105 - BV421
5.7
4.2
9.7
8.2
4.0
3.3
8.9
64
38
26
2.3
25
43
42
15
58
47
44
B
CD105pos v CD105neg
RhoGDI signaling
GPCR-Mediated Nutrient Sensing in Enteroendocrine Cells
White adipose tissue browning pathway
p value (-log10)
Pathway activation score
Signaling by Rho-family GTPases
NFκB activation by viruses
HGF signaling
ErbB signaling
Natural killer cell signaling
C
Col1a1
Pdpn
CAFs
Pericytes
Acta2 (αSMA)
Eng (CD105)
CD105neg CAFs
CD105pos CAFs
High
mRNA expression
Low
D
Cxcl14
Col8a1
Ltbp2
Postn
Fap
Ly6c1
H2-Ab1
Cd74
Saa3
Msln
Upk3b
Krt18
E
Hu norm. adj. panc and PDA
All cells
COL1A1
ACTA2 (αSMA)
Extract fibroblast/pericyte clusters, re-cluster
Hu norm. adj. panc and PDA
Fibroblasts and pericytes only
RGS5
Extract fibroblast clusters and analyse
Hu norm. adj. panc and PDA
Fibroblasts only
F
ENG
Norm. mRNA Expression
Identity
G
COL1A1
ACTA2
PDGFRA
CXCL14
GAS1
ENG
TAGLN
C3
LTBP2
SOD2

Supplemental Figure 4, related to Figure 3. CD105 expression discriminates two distinct CAF populations in murine and human PDA

(A) FACS gating used to isolate EpCAM^{neg} CD31^{neg} CD45^{neg} CD90^{pos} PDPN^{pos} - CD105^{pos} (n=6) and - CD105^{neg} (n=6) PDA CAFs. L/D: Live/Dead, LIN: EpCAM CD31 CD45. Scatter gating for singlets is not shown.

(B) Ingenuity Pathway Analysis (IPA) of isolated PDA CAF gene expression, displaying pathway activation score. Displaying plots for positively enriched (enriched in CD105^{pos}, yellow) (B) and negatively enriched (enriched in CD105^{neg}, purple) (C).

(C-D) Reanalysis of single cell transcriptomic data from Elyada et al. The pre-defined fibroblast enriched fraction was used and only collagen expressing cells analyzed. Data is displayed as UMAP projections with overlaid expression levels of example genes, including canonical fibroblast genes (*Col1a1*, *Pdpn*, *Acta2*) and Eng (the gene that encodes CD105) (C), genes with increased expression in CD105^{pos} PDA CAFs (*Cxcl14*, *Col8a1*, *Ltbp2*, *Postn*, *Fap* and *Ly6c1*) and gene with increased expression in CD105^{neg} PDA CAFs (*H2Ab1*, *Cd74*, *Saa3*, *Msln*, *Up3kb* and *Krt18*) (D).

(E) Single cell transcriptomic analysis of human (Hu) PDA tumor (n=14) and normal adjacent (norm adj) (n=2) (Steele et al., 2020). Displayed as UMAP projections with the expression levels of listed genes overlaid. The method for extracting fibroblast cells is shown using example genes to navigate appropriate clusters. Fibroblast clusters are visualized by color-coding (right).

(F) Violin plots displaying *ENG* expression levels (standard Seurat normalized) of the fibroblast clusters from (E). Plots display maximum and minimum data range with width representing probability density.

(G) UMAP projection of fibroblasts from (E), with overlaid expression of *COL1A1* and ENG, myCAF-associated genes (*ACTA2* and *TAGLN*), iCAF-associated genes (*PDGFRA* and *C3*), example CD105^{pos} fibroblast signature genes (*CXCL14* and *LTBP2*) and example CD105^{neg} fibroblast signature genes (*GAS1* and *SOD2*).

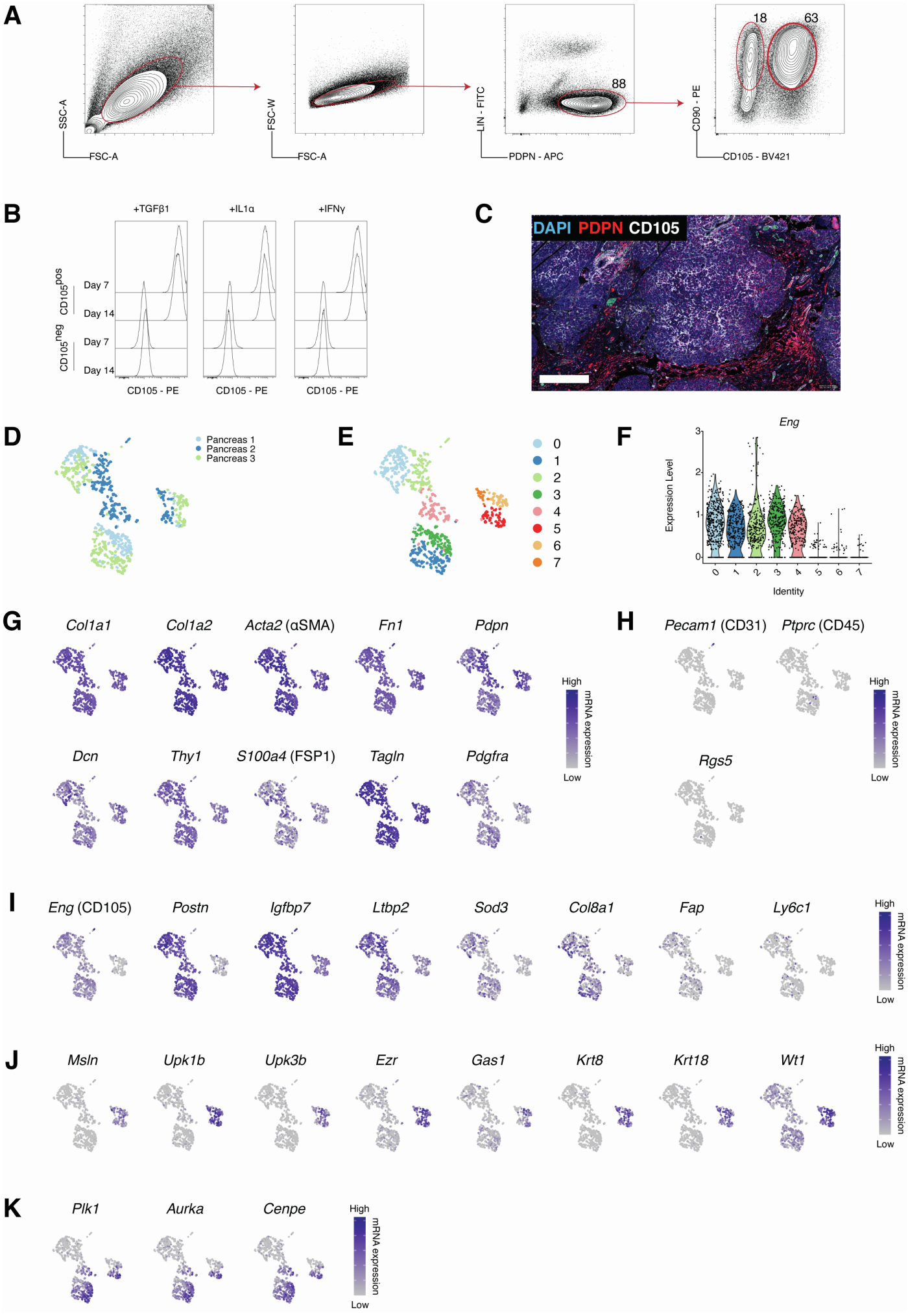
A
SSC-A
FSC-A
FSC-W
FSC-A
LIN - FITC
PDPN - APC
88
CD90 - PE
CD105 - BV421
18
63
B
+TGFβ1
+IL1α
+IFNγ
CD105pos
CD105neg
Day 7
Day 14
Day 7
Day 14
CD105 - PE
CD105 - PE
CD105 - PE
C
DAPI PDPN CD105
D
Pancreas 1
Pancreas 2
Pancreas 3
E
0
1
2
3
4
5
6
7
F
Eng
Expression Level
Identity
G
Col1a1
Col1a2
Acta2 (αSMA)
Fn1
Pdpn
Dcn
Thy1
S100a4 (FSP1)
Tagln
Pdgfra
High
mRNA expression
Low
H
Pecam1 (CD31)
Ptprc (CD45)
Rgs5
High
mRNA expression
Low
I
Eng (CD105)
Postn
Igfbp7
Ltbp2
Sod3
Col8a1
Fap
Ly6c1
High
mRNA expression
Low
J
Msln
Upk1b
Upk3b
Ezr
Gas1
Krt8
Krt18
Wt1
High
mRNA expression
Low
K
Plk1
Aurka
Cenpe
High
mRNA expression
Low

Supplemental Figure 5, related to Figure 4. Phenotypic plasticity of mesenchymal marker expression

(A) Representative FACS gating strategy to isolate $CD105^{pos}$ and $CD105^{neg}$ pancreatic fibroblasts (PaFs) after 7 days of *in vitro* expansion from normal healthy pancreas. L/D: Live/Dead, LIN: EpCAM CD31 CD45. Plots are representative of n=8 experiments.

(B) Flow cytometry analysis of CD105 in populations of purified $CD105^{pos}$ and $CD105^{neg}$ PaFs after 7 and 14 days in culture with TGFβ1, IL1α or IFNγ. Plots are representative of n=4 experiments.

(C) Representative immunohistochemistry (IHC) analysis of normal but inflamed human pancreas tissue, adjacent to PDA tumors. Stained with DAPI (blue) and with antibodies targeting podoplanin (PDPN) (red) and CD105 (white). Scale bar = 750 µm.

(D-J) Single cell transcriptomic analysis of *in vitro* expanded fibroblasts from healthy mouse pancreas (n=3), after 7 days of culture (same time point for the FACS isolation described in (A)). Displayed as UMAP projections (D, E, G-K). Comparison of the n=3 samples demonstrates concordant results (D). Clusters are defined in (E) and *Eng* gene expression in each cluster displayed (F). Expression levels of example genes are overlaid, including canonical fibroblast genes (G), canonical genes of endothelial, immune and perivascular cells (H), *Eng* and other $CD105^{pos}$ fibroblast signature genes (I), $CD105^{neg}$ signature and mesothelial-associated genes (J) and cell cycle-associated genes (K).

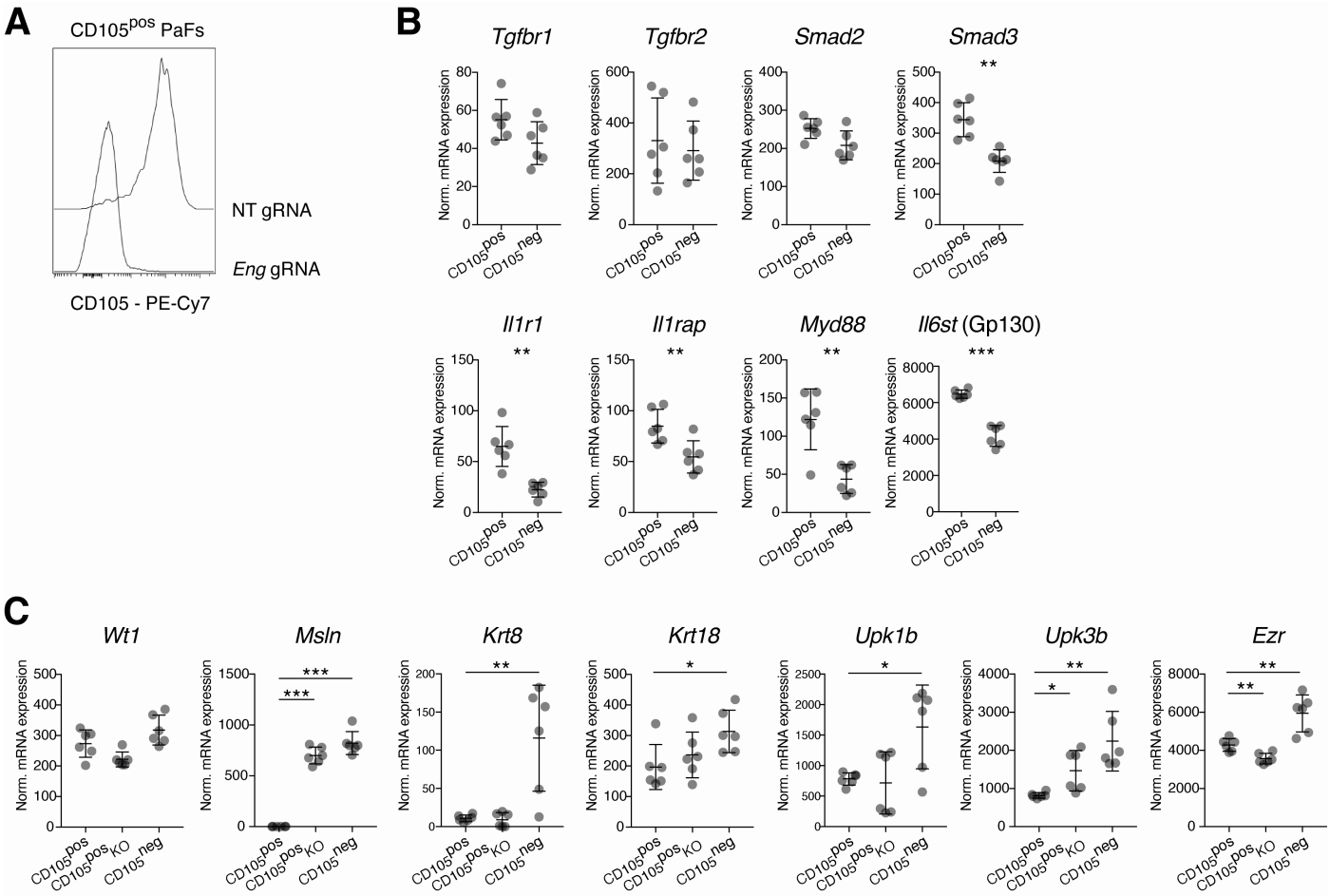
A
CD105pos PaFs
NT gRNA
Eng gRNA
CD105 - PE-Cy7
B
Tgfbr1
Tgfbr2
Smad2
Smad3
Il1r1
Il1rap
Myd88
Il6st (Gp130)
Norm. mRNA expression
CD105pos
CD105neg
C
Wt1
Msln
Krt8
Krt18
Upk1b
Upk3b
Ezr
CD105pos
CD105posKO
CD105neg

Supplemental Figure 6, related to Figure 5. Differential signaling engagement of CD105^{pos} and CD105^{neg} PaFs

(A) Flow cytometry validation of knockout of cell surface CD105 in CD105^{pos} pancreatic fibroblasts (PaFs) by CRISPR-Cas-9 gene editing.

(B) mRNA expression of genes associated with TGFβ signal transduction (*Tgfrb1*, *Tgfbr2*, *Smad2* and *Smad3*), IL1 signal transduction (*Il1r1*, *Il1rap* and *Myd88*) and *Il6st* (Gp130) in CD105^{pos} (n=6) and CD105^{neg} (n=6) PaFs. Gene expression measured by RNA-seq and quantified as DEseq2 median ratio normalized expression values. Displaying expression values as mean±standard deviation (SD).

(C) mRNA expression of genes associated with mesothelial identity in CD105^{pos}, CD105^{pos} KO and CD105^{neg} PaFs, Gene expression measured by RNA-seq and quantified as DEseq2 median ratio normalized expression values. Displaying expression values as mean±standard deviation (SD).

Samples are compared using unpaired t-test (B-C). ns. non-significant, *p<0.05, **p<0.01, ***p<0.001.

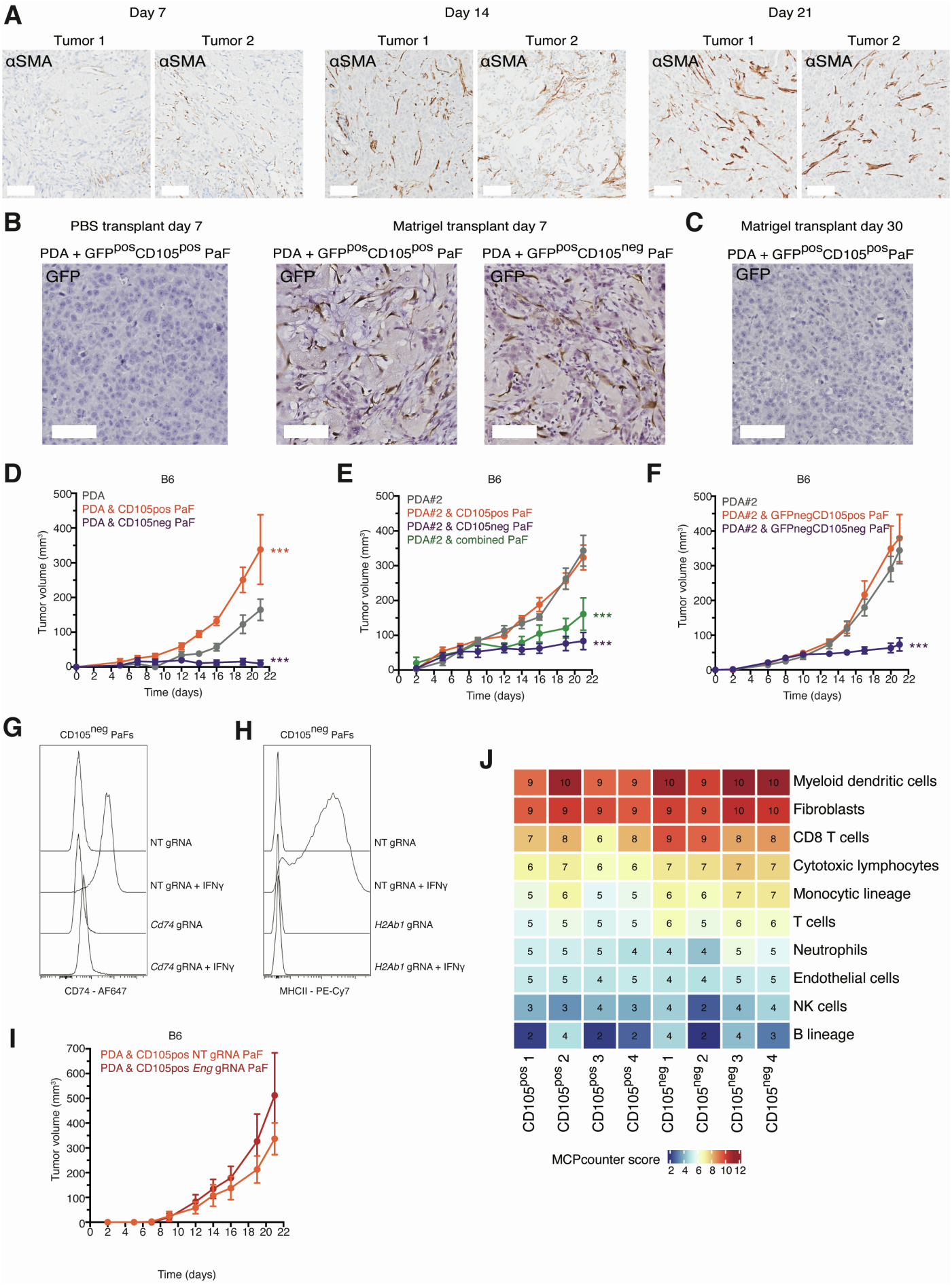
A
Day 7
Day 14
Day 21
Tumor 1
Tumor 2
αSMA
B
PBS transplant day 7
Matrigel transplant day 7
PDA + GFPposCD105pos PaF
PDA + GFPposCD105neg PaF
GFP
C
Matrigel transplant day 30
PDA + GFPposCD105posPaF
D
B6
PDA
PDA & CD105pos PaF
PDA & CD105neg PaF
Tumor volume (mm3)
Time (days)
***
E
PDA#2
PDA#2 & CD105pos PaF
PDA#2 & CD105neg PaF
PDA#2 & combined PaF
F
PDA#2 & GFPnegCD105pos PaF
PDA#2 & GFPnegCD105neg PaF
G
CD105neg PaFs
NT gRNA
NT gRNA + IFNγ
Cd74 gRNA
Cd74 gRNA + IFNγ
CD74 - AF647
H
H2Ab1 gRNA
H2Ab1 gRNA + IFNγ
MHCII - PE-Cy7
I
PDA & CD105pos NT gRNA PaF
PDA & CD105pos Eng gRNA PaF
J
Myeloid dendritic cells
Fibroblasts
CD8 T cells
Cytotoxic lymphocytes
Monocytic lineage
T cells
Neutrophils
Endothelial cells
NK cells
B lineage
CD105pos 1
CD105pos 2
CD105pos 3
CD105pos 4
CD105neg 1
CD105neg 2
CD105neg 3
CD105neg 4
MCPcounter score

Supplemental Figure 7, related to Figure 6. CD105^{neg} fibroblasts restrict tumor growth *in vivo*

(A) Immunohistochemistry (IHC) of subcutaneous tumors from mono-transplanted KPC PDA tumor cells in Matrigel at indicated time points. Stained with an αSMA targeting antibody and Haematoxylin. Represetative of n=4-5 tumors. Scale bar = 80 µm.

(B) IHC of subcutaneous tumors from co-transplanted KPC PDA tumor cells and GFP^{pos} pancreatic fibroblasts (PaFs) into syngeneic B6 mice. Stained with a GFP targeting antibody and Haematoxylin. No GFP^{pos} fibroblasts are observed in the growing tumors after 7 days when the cells are injected in PBS (left) but are highly abundant in growing tumors in which cells are injected in Matrigel (right). Scale bar = 80 µm.

(C) No GFP^{pos} fibroblasts are retained 30 days after KPC PDA tumor cells and GFP^{pos} PaFs are co-transplanted. This likely represents a limitation of this model for studies of long-term cancer cell and fibroblast interactions *in vivo*.

(D-F) Tumor growth of subcutaneous injection of 10^5 PDA tumor cells or co-transplantation with 10^5 CD105^{pos} or CD105^{neg} pancreatic fibroblasts (PaFs) in syngeneic B6 mice. Shown are independent experiment from Figure 6B (D), with alternative KPC PDA cell line from a fully backcrossed B6 mouse (E) and with PaFs with no GFP expression (F). n=5 mice per condition.

(G, H) Flow cytometry validation of CD74 (I) and MHCII (J) knock out in CD105^{neg} PaFs by CRISPR-Cas-9 gene editing.

(I) Tumor growth of subcutaneous injection of 10^5 PDA tumor cells co-transplanted with 10^5 CD105^{pos} PaFs with Eng expression disrupted by CRISPR-Cas-9 gene editing. CD105^{pos} PaFs transfected with non-targeting (NT) gRNAs are used as control. n=5 mice per condition.

(J) MCPcounter analysis of bulk gene expression profiles of subcutaneous KPC PDA and CD105^{pos} PaFs or CD105^{neg} PaF co-transplanted tumors at day 10.

Data is displayed as mean tumor volumes±standard error of the mean (SEM) (D-F and I).

Conditions are compared using 2-way ANOVA (B-G). *p<0.05, **p<0.01, ***p<0.001.

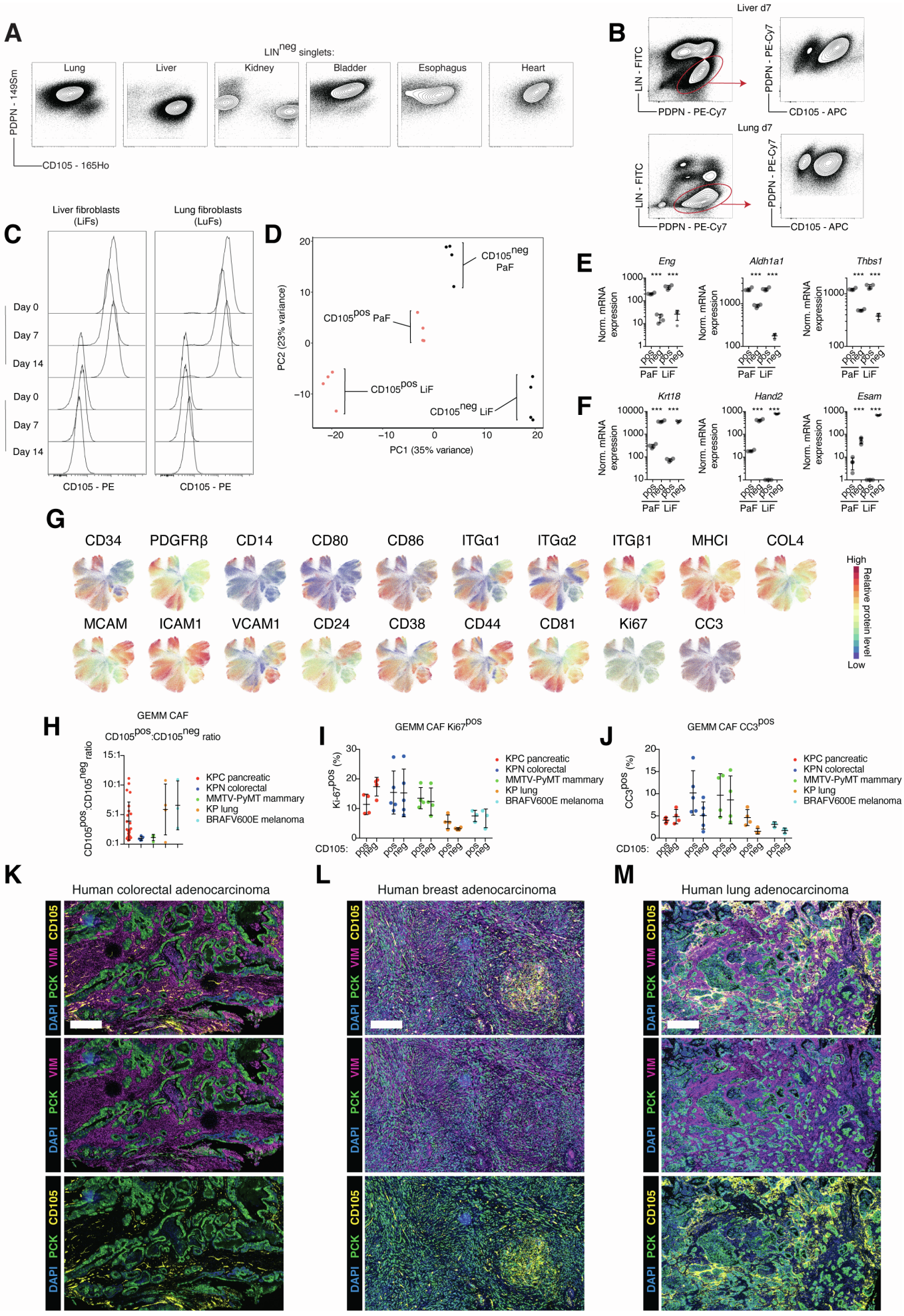
A
LIN^neg singlets:
Lung
Liver
Kidney
Bladder
Esophagus
Heart
PDPN - 149Sm
CD105 - 165Ho
B
Liver d7
LIN - FITC
PDPN - PE-Cy7
PDPN - PE-Cy7
CD105 - APC
Lung d7
LIN - FITC
PDPN - PE-Cy7
PDPN - PE-Cy7
CD105 - APC
C
Liver fibroblasts (LiFs)
Lung fibroblasts (LuFs)
CD105^pos isolation
Day 0
Day 7
Day 14
CD105^neg isolation
Day 0
Day 7
Day 14
CD105 - PE
CD105 - PE
D
CD105^neg PaF
CD105^pos PaF
CD105^pos LiF
CD105^neg LiF
PC2 (23% variance)
PC1 (35% variance)
E
Eng
Aldh1a1
Thbs1
Norm. mRNA expression
pos neg pos neg pos neg
PaF LiF
F
Krt18
Hand2
Esam
Norm. mRNA expression
pos neg pos neg pos neg
PaF LiF
G
CD34
PDGFRβ
CD14
CD80
CD86
ITGα1
ITGα2
ITGβ1
MHCI
COL4
MCAM
ICAM1
VCAM1
CD24
CD38
CD44
CD81
Ki67
CC3
High
Relative protein level
Low
H
GEMM CAF
CD105^pos:CD105^neg ratio
CD105^pos:CD105^neg ratio
15:1
10:1
5:1
0:1
KPC pancreatic
KPN colorectal
MMTV-PyMT mammary
KP lung
BRAFV600E melanoma
I
GEMM CAF Ki67^pos
Ki-67^pos (%)
CD105: pos neg pos neg pos neg pos neg pos neg
KPC pancreatic
KPN colorectal
MMTV-PyMT mammary
KP lung
BRAFV600E melanoma
J
GEMM CAF CC3^pos
CC3^pos (%)
CD105: pos neg pos neg pos neg pos neg pos neg
KPC pancreatic
KPN colorectal
MMTV-PyMT mammary
KP lung
BRAFV600E melanoma
K
Human colorectal adenocarcinoma
DAPI PCK VIM CD105
DAPI PCK VIM
DAPI PCK CD105
L
Human breast adenocarcinoma
DAPI PCK VIM CD105
DAPI PCK VIM
DAPI PCK CD105
M
Human lung adenocarcinoma
DAPI PCK VIM CD105
DAPI PCK VIM
DAPI PCK CD105

Supplemental Figure 8, related to Figure 7. CD105^{pos} and CD105^{neg} fibroblasts are identified in normal and tumor-bearing tissues

(A) Mass cytometry (MC) analysis of *in vitro* expanded, low passage, primary fibroblast isolations from mouse organs not displayed in Figure 7A. Cells expressing canonical markers of epithelial, immune, endothelial and perivascular cells are excluded from the analysis and live, singlets are displayed in plots showing PDPN and CD105 levels. LIN: EpCAM CD45 CD31

(B) Flow cytometry analysis of EpCAM^{neg} CD45^{neg} CD31^{neg} (LIN^{neg}) and PDPN^{pos} liver (top) and lung (bottom) fibroblasts from day 7 primary cell isolations, an earlier time-point than the analysis of these isolations by MC in Figure 7A and Figure S7A.

(C) Flow cytometry analysis of purified and CD105^{pos} and CD105^{neg} liver (LiF) and lung (LuF) fibroblasts after 1 and 2 weeks of *in vitro* culture. Plots are representative of n=4 experiments.

(D) Principle component (PC) analysis of differentially expressed genes between *in vitro* expanded CD105^{pos} and CD105^{neg} LiFs and pancreatic fibroblasts (PaFs).

(E-F) mRNA expression of genes associated with CD105 expression in liver and pancreatic fibroblasts. Gene expression measured by RNA-seq and quantified as DEseq2 median ratio normalized expression values. Displaying expression values as mean ± standard deviation (SD).

(G) UMAP projection from Figure 7B, displaying relative intensity of additional phenotypic markers not included in Figure 7F.

(H) MC analysis of the ratio of CD105^{pos}:CD105^{neg} CAFs in tumors from genetically engineered mouse models (GEMMs) of pancreatic (KPC) (n=23), colorectal (KPN) (n=5), mammary (MMTV-PyMT) (n=4), lung (KP) (n=4) and melanoma (BRAF^{v600E}) (n=3) cancer. Data from the n=19 PDA tumor samples analyzed in Figure 1 were combined to increase the accuracy of the ratio measured for the pancreatic GEMM tumors. Displayed as mean ± standard deviation (SD).

(I-J) MC analysis of proliferation (I) and apoptosis (J) rates of CD105^{pos} and CD105^{neg} GEMM CAFs. n=5 tumors for each genotype (paired CD105^{pos} and CD105^{neg} fractions). Displayed as mean ± SD.

(K-M) Immunohistochemistry (IHC) analysis of additional representative human colorectal (K), breast (L) and lung adenocarcinoma (M) tumor samples stained for pan-cytokeratin (PCK) (green), vimentin (VIM) (purple), CD105 (yellow) and DAPI (blue). Scale bar = 500 μm.